Structure and Chemical State of the Pt(557) Surface during Hydrogen Oxidation Reaction Studied by in Situ Scanning Tunneling Microscopy and X-ray Photoelectron Spectroscopy

7 AUTHORS, INCLUDING:

Gérôme Melaet
University of California, Berkeley
16 PUBLICATIONS   **196** CITATIONS

SEE PROFILE

Stephanus Axnanda
BASF SE
35 PUBLICATIONS   **511** CITATIONS

SEE PROFILE

Selim Alayoglu
Lawrence Berkeley National Laboratory
60 PUBLICATIONS   **1,901** CITATIONS

SEE PROFILE

Zhi Liu
ShanghaiTech University
189 PUBLICATIONS   **3,184** CITATIONS

SEE PROFILE

Structure and Chemical State of the Pt(557) Surface during Hydrogen Oxidation Reaction Studied by in Situ Scanning Tunneling Microscopy and X-ray Photoelectron Spectroscopy

Zhongwei Zhu,[†,‡] Gérôme Melaet,[†,§] Stephanus Axnanda,[∥] Selim Alayoglu,[†,§] Zhi Liu,[∥] Miquel Salmeron,*[,‡,⊥] and Gabor A Somorjai*[,†,‡]

[†]Department of Chemistry, University of California, Berkeley, California, 94720, United States United States

[‡]Materials Sciences Division, Lawrence Berkeley National Laboratory, Berkeley, California, 94720, United States United States

[§]Chemical Sciences Division, Lawrence Berkeley National Laboratory, Berkeley, California, 94720, United States United States

[∥]Advanced Light Source, Lawrence Berkeley National Laboratory, Berkeley, California, 94720, United States United States

[⊥]Department of Materials Science and Engineering, University of California, Berkeley, California, 94720, United States United States

S *Supporting Information*

ABSTRACT: The surface structure of Pt(557) during the catalytic oxidation of hydrogen was studied with *in situ* scanning tunneling microscopy and X-ray photoelectron spectroscopy. At 298 K, the surface Pt oxide formed after exposing Pt(557) to approximately 1 Torr of O_2 can be readily removed by H_2, at H_2 partial pressures below 50 mTorr. Water is detected as the product in the gas phase, which also coadsorbs with hydroxyl groups on the Pt(557) surface.

A crucial question in heterogeneous catalysis involves the dependence of catalytic reactivity on the structure of the catalyst−reactant interface, and the identification of reaction intermediates and surface sites responsible for turnovers. The development of *in situ* techniques has provided great opportunities to explore these questions, by bridging the over 9 orders of magnitude pressure gap between traditional model catalytic studies (below 10^{-6} Torr) and industrial catalysis (at or above atmospheric pressures). High-pressure scanning tunneling microscopy (HP-STM) is a unique tool to investigate the catalyst surface structure at the molecular level[1−9] and the highly mobile nature of atoms and molecules on catalytically active surfaces.[10−12] Spectroscopic techniques, particularly ambient-pressure X-ray photoelectron spectroscopy (AP-XPS), yield information regarding surface composition and oxidation states of surface species during reactions.[8−10,13−16]

Catalyst surfaces can undergo dramatic reconstruction in response to changes in gas composition during catalytic reactions.[4,11,15−18] For example, Pt oxide is formed during CO oxidation on Pt(110) under O_2-rich conditions along with high activity.[4] Switching the gas mixture into a CO-rich environment leads to the reduction of the Pt(110) surface and simultaneously a strong decrease in activity. Here we examine the structure of the stepped Pt(557) surface during the hydrogen oxidation reaction and the evolution of Pt oxide that forms on Pt(557) under pure O_2.[19] When H_2 is oxidized by O_2 at Pt surfaces in vacuum above 170 K (water desorption temperature), the formation of hydroxyl groups (OH) through

hydrogenation of chemisorbed oxygen atoms is the rate-limiting step:[20−22]

$$O(a) + H(a) \rightarrow OH(a) \tag{1}$$

$$OH(a) + H(a) \rightarrow H_2O(a) \rightarrow H_2O(g) \tag{2}$$
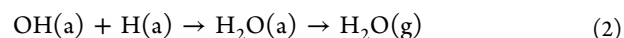
This reaction is autocatalytic below 170 K in vacuum, since, in the presence of adsorbed water molecules, OH species can be produced through alternative reaction channels:[20−22]

$$H_2O(a) + O(a) \rightarrow 2OH(a) \tag{3}$$

$$2H_2O(a) + O(a) \rightarrow 2OH(a) + H_2O(a)$$
$$\rightarrow 3OH(a) + H(a) \tag{4}$$
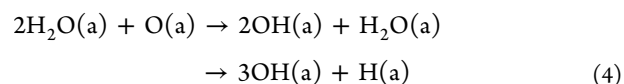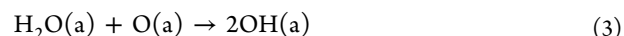
Despite these well-known mechanisms of hydrogen oxidation at low temperatures in vacuum, the mechanism under ambient pressures and temperatures is not well understood at the molecular scale. The formation of Pt oxide, which can be stabilized at sufficiently high O_2 pressures, adds another parameter that needs to be considered.

With HP-STM and AP-XPS, we investigate the structure and chemical state of the Pt(557) surface under an O_2 partial pressure near 1 Torr and H_2 partial pressures below 50 mTorr. The removal of Pt oxide clusters with the increase of H_2 partial pressures is monitored by HP-STM. AP-XPS has revealed that water is the reaction product in the gas phase and that water coadsorbs with hydroxyl groups on Pt(557).

STM measurements were performed in a home-built instrument containing a gold-coated high-pressure batch cell wherein gases are introduced.[23] The cell resides inside an ultrahigh vacuum (UHV) system where the Pt(557) sample is prepared and transferred without loss of vacuum. AP-XPS spectra were recorded at Beamline 9.3.2 at the Advanced Light Source at Lawrence Berkeley National Laboratory.[24] The Pt(557) crystal was cleaned via cycles of Ar$^+$ bombardment, annealing in O_2, and flashing to 1073 K in vacuum, as in our
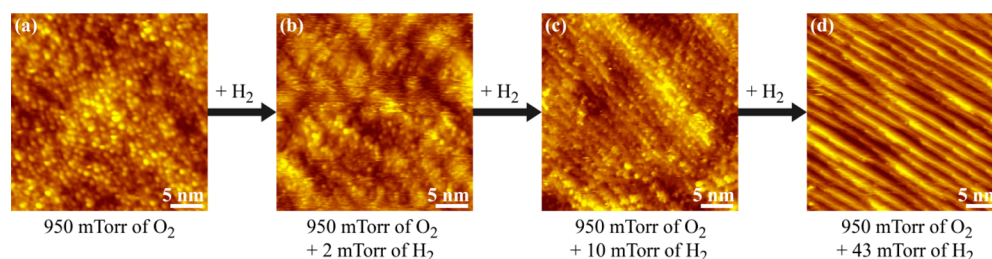
Figure 1. STM images of the Pt(557) surface at 298 K. (a) Under 950 mTorr of O_2, the surface is covered by Pt oxide clusters approximately 1 nm in diameter. The clusters are roughly aligned along the step edges. (b−d) Under a mixture of 950 mTorr of O_2 and (b) 2 mTorr, (c) 10 mTorr, and (d) 43 mTorr of H_2, the coverage of Pt oxide decreases with increasing H_2 partial pressures until the Pt oxide clusters ultimately disappear.

previous studies.[3,19] The cleaning procedures were repeated until the level of contaminants was below the sensitivity of Auger Electron Spectroscopy for HP-STM experiments and below the sensitivity of XPS for AP-XPS measurements. O_2 and H_2 were introduced separately through leak valves. All the HP-STM and AP-XPS experiments were carried out at 298 K.

Under pure O_2, the Pt(557) surface is covered by ~1 nm large clusters that are roughly aligned along the original step edges, as shown in Figure 1a. These clusters were previously identified as surface Pt oxide.[19] H_2 was added after the cluster overlayer had formed under O_2. The structural evolution of the Pt(557) surface with increasing H_2 partial pressures is monitored with STM and displayed in Figure 1. The Pt oxide clusters are still distinguishable in the STM image after introducing 2 mTorr of H_2 (Figure 1b). At a higher H_2 partial pressure of 10 mTorr, the coverage of Pt oxide clusters becomes much smaller, with most of the remaining clusters present at the Pt step edges (Figure 1c). When the H_2 partial pressure reaches 43 mTorr, the Pt oxide clusters have completely disappeared and Pt steps are restored (Figure 1d). Since these clusters can be readily removed at a low H_2/O_2 pressure ratio of 1:20, the high reactivity of Pt oxide toward H_2 agrees with literature reports that Pt oxide is active in hydrogen oxidation.[25−27] An induction period ranging from 10 to 80 min was reported for the reaction involving Pt oxide as the catalyst, with the length depending on the preparation of Pt oxide.[25] The imaging was started 15 min after introducing gases, and we did not observe any changes in the surface structure with reaction time. Accordingly, the induction period in our experiments, if it exists, should be shorter than 15 min.

The Pt(557) surface structure under pure H_2 was also investigated as a reference for understanding the structural changes in Figure 1. STM images reveal that the stepped structure is preserved when Pt(557) is exposed to 100 mTorr of H_2 at 298 K (Figure S2a). The average terrace width is 1.4 nm, the same value as the terrace width of clean Pt(557) in UHV. Interestingly, step edges are frizzy under 100 mTorr of H_2, which indicates an enhanced mobility of the Pt step atoms, probably by virtue of the attachment of hydrogen atoms. No changes in the stepped structure were observed when the H_2 pressure was increased to 1 Torr (Figure S2b). Only an increase in the noise level was observed, probably as a consequence of enhanced surface mobility. Therefore, unlike CO and O_2, H_2 does not induce cluster formation or step coalescence on Pt(557).

In situ XPS experiments were performed under similar gas environments as in the HP-STM measurements, in order to examine the chemical state of Pt(557) during the structural evolution. Pt 4f and O 1s core level spectra were recorded at X-ray photon energies of 340 and 810 eV, which generate

photoelectrons with kinetic energies of 270−280 eV and thus ensure a similar probing depth of ~0.6 nm for both elements.[28] Binding energies were calibrated with respect to the Fermi edge fixed at 0 eV in the valence band region acquired under the same conditions. The O 1s spectra are displayed in Figure 2
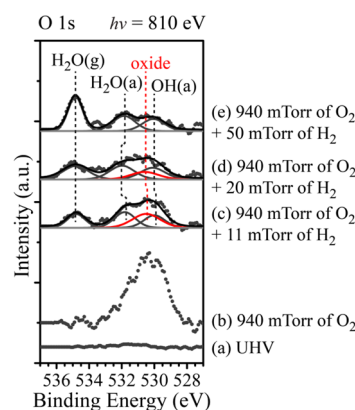

Figure 2. O 1s spectra of Pt(557) acquired at 298 K with an incident X-ray photon energy of 810 eV (a) in UHV, (b) under 940 mTorr of O_2, and after addition of H_2 at partial pressures of (c) 11, (d) 20, and (e) 50 mTorr. The O 1s peaks of gas-phase O_2 characterized by a doublet at 538.4 and 539.5 eV are outside the range of the figure. The deconvoluted spectra illustrate how the introduction of H_2 results in the progressive decrease and the final disappearance of surface Pt oxide (red). Water is formed in the gas phase upon the introduction of H_2.

with the intensities normalized to the Pt 4f peak intensities under identical conditions. The gas-phase O_2 doublet peak (not shown) is located at 538.4 and 539.5 eV. A wide peak appears at ~530.5 eV after filling the chamber with 940 mTorr of O_2. This peak, with full width at half-maximum (fwhm) of 2.5 eV, is mainly due to the Pt oxide clusters covering the Pt(557) surface. Two other surface components may also contribute to the peak: chemisorbed oxygen that gives rise to a peak at 529.9 eV,[19] and OH groups formed by reactions with H_2 in the vacuum background gas, which produces peaks around 531 eV.[29−31] After the introduction of H_2, a new peak at 534.9 eV due to gas-phase water[32−34] appears and grows with H_2 partial pressures, indicating that water is the product.

Meanwhile, the intensity of the initial surface Pt oxide peak greatly decreases with the addition of H_2, concomitant with the decrease in oxide cluster coverage in STM images. Significant changes in the O 1s peak shape are also observed, indicating the formation of various O-related species. In order to analyze the surface chemical states, the O 1s spectra in Figure 2c−e recorded under the H_2−O_2 mixture were deconvoluted using the gas-phase water peak and three surface components. The

surface components include the Pt oxide peak at ~530.5 eV as in Figure 2b, chemisorbed H_2O peak at ~531.9 eV, and chemisorbed OH peak at ~530.1 eV. The assignment of chemisorbed H_2O and OH peaks agrees with literature values[30,31] and a recent study by Nilsson et al.,[35] where O 1s binding energies of chemisorbed H_2O and OH are 531.7 and 530.3 eV when they bond to each other. When the H_2 partial pressure reaches 50 mTorr (Figure 2e), the H_2O and OH peaks are sufficient for a good fit. The absence of the surface Pt oxide component agrees with STM results that Pt oxide clusters are removed at H_2 partial pressures above 43 mTorr. In addition, under our conditions of water and H_2 gas phase in the mTorr range, little chemisorbed oxygen can be present at the Pt(557) surface, since adsorbed H_2O molecules readily react with chemisorbed oxygen atoms to form OH species through reactions 3 and 4, which are fast enough to proceed at ambient temperatures.[21]

Under a H_2 partial pressure of 11 to 20 mTorr (Figure 2c,d), the surface Pt oxide component at 530.5 eV needs to be included in the deconvolution of O 1s spectra for a good fit. Because O 1s peaks of Pt oxide and OH groups are separated by only 0.4 eV, their relative intensity ratio can largely vary with slight changes in fitting parameters. To remedy this problem, the ratio of the chemisorbed H_2O to OH peak areas was constrained to a fixed value—the ratio in the spectrum under 940 mTorr of O_2 and 50 mTorr H_2, when Pt oxide is absent. The deconvolution results show that the surface Pt oxide peak, marked by red curves, declines and ultimately disappears with the addition of H_2, along with the growth of the gas-phase water peak. In contrast, the peaks of chemisorbed H_2O and OH retain their intensities during the reaction. Hydrogen atoms, which cannot be detected by STM or XPS in our experiments, are also likely to chemisorb on the Pt(557) surface during the reaction. Diffusion of hydrogen into subsurface sites, which typically happens on Pd surfaces,[36] cannot happen because the energy barrier for hydrogen atoms to diffuse into the subsurface is 0.66 and 0.99 eV on Pt(111) and Pt(100), respectively.[37,38] Such high activation energies should strongly inhibit hydrogen diffusion into the subsurface at 298 K.

The total amount of surface oxygen, i.e. the oxygen coverage, can be estimated from the ratio of integrated areas of all surface O 1s peaks to Pt 4f peaks. Peak areas from 0.25 ML oxygen on Pt(111) at 10^{-7} Torr are used to calibrate the coverage.[39,40] Figure 3 shows that, as the H_2 partial pressure increases, the oxygen coverage decreases rapidly and the amount of water in the gas phase increases rapidly while oxide is present at the surface. Starting at 0.92 ML on the oxide-covered surface under 940 mTorr of O_2, the oxygen coverage sharply drops to 0.34 ML after 11 mTorr of H_2 is introduced, accompanied by a sharp increase in the area of the gas-phase water peak. The oxygen coverage drops to 0.31 ML after raising the H_2 partial pressure to 20 mTorr, and further to 0.21 ML after adding 50 mTorr of H_2 which completely removes all the surface Pt oxide. Along with a moderate decline in oxygen coverage, the growth of the water gas peak also becomes slower. In addition, the total coverage of chemisorbed H_2O and OH stays at ~0.21 ML under all three H_2 partial pressures, indicating that the removal of Pt oxide is exclusively responsible for the drop in oxygen coverage by reaction with H_2.

In summary, the surface Pt oxide on Pt(557) formed under approximately 1 Torr of O_2 is highly reactive to H_2. The effects of the hydrogen oxidation reaction were visible by STM at a low H_2 partial pressure of 2 mTorr. When raising the H_2 partial
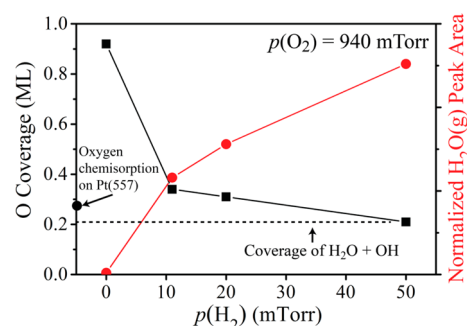

Figure 3. Changes in total oxygen coverage on Pt(557) (black squares) and normalized water gas peak area (red circles) with H_2 partial pressures when keeping the O_2 partial pressure at 940 mTorr at 298 K. Reactions between Pt oxide and H_2 are responsible for the initial rapid decrease in the oxygen coverage and the initial increase in the normalized gas-phase water peak area. The total coverage of chemisorbed H_2O and OH remains constant at ~0.21 ML above 11 mTorr of H_2.

pressure, the smaller amount of Pt oxide visible in the STM images and the weaker oxide peak in O 1s spectra illustrate that the reaction proceeds via consumption of Pt oxide, whereas the amount of chemisorbed H_2O and OH species remains constant at ~0.21 ML. Ultimately, at H_2 partial pressures greater than 43 mTorr, the surface Pt oxide is fully removed.

■ ASSOCIATED CONTENT

Ⓢ Supporting Information

Additional STM images of Pt(557) under pure H_2 and H_2–O_2 mixture, Pt 4f spectra, C 1s spectra, parameters of peak fitting, and O 1s spectra of Pt(557) under H_2O. This material is available free of charge via the Internet at http://pubs.acs.org.

■ AUTHOR INFORMATION

Corresponding Author

mbsalmeron@lbl.gov (M.S.); somorjai@berkeley.edu (G.A.S.)

Notes

The authors declare no competing financial interest.

■ REFERENCES

(1) Besenbacher, F.; Thostrup, P.; Salmeron, M. *MRS Bull.* **2012**, *37*, 677−681.

(2) Vang, R. T.; Lauritsen, J. V.; Lægsgaard, E.; Besenbacher, F. *Chem. Soc. Rev.* **2008**, *37*, 2191−2203.

(3) Tao, F.; Dag, S.; Wang, L. W.; Liu, Z.; Butcher, D. R.; Bluhm, H.; Salmeron, M.; Somorjai, G. A. *Science* **2010**, *327*, 850−853.

(4) Hendriksen, B. L. M.; Frenken, J. W. M. *Phys. Rev. Lett.* **2002**, *89*, 046101.

(5) Longwitz, S. R.; Schnadt, J.; Vestergaard, E. K.; Vang, R. T.; Lægsgaard, E.; Stensgaard, I.; Brune, H.; Besenbacher, F. *J. Phys. Chem. B* **2004**, *108*, 14497−14502.

(6) Österlund, L.; Rasmussen, P. B.; Thostrup, P.; Lægsgaard, E.; Stensgaard, I.; Besenbacher, F. *Phys. Rev. Lett.* **2001**, *86*, 460−463.

(7) Zhu, Z.; Butcher, D. R.; Mao, B.; Liu, Z.; Salmeron, M.; Somorjai, G. A. *J. Phys. Chem. C* **2013**, *117*, 2799−2804.

(8) Butcher, D. R.; Grass, M. E.; Zeng, Z.; Aksoy, F.; Bluhm, H.; Li, W.-X.; Mun, B. S.; Somorjai, G. A.; Liu, Z. *J. Am. Chem. Soc.* **2011**, *133*, 20319−20325.

(9) Merte, L. R.; Knudsen, J.; Eichhorn, F. M.; Porsgaard, S.; Zeuthen, H.; Grabow, L. C.; Lægsgaard, E.; Bluhm, H.; Salmeron, M.; Mavrikakis, M.; Besenbacher, F. *J. Am. Chem. Soc.* **2011**, *133*, 10692−10695.

(10) Montano, M.; Bratlie, K. M.; Salmeron, M.; Somorjai, G. A. *J. Am. Chem. Soc.* **2006**, *128*, 13229−13234.

(11) Vestergaard, E. K.; Vang, R. T.; Knudsen, J.; Pedersen, T. M.; An, T.; Lægsgaard, E.; Stensgaard, I.; Hammer, B.; Besenbacher, F. *Phys. Rev. Lett.* **2005**, *95*, 126101.

(12) Butcher, D. R.; Zhu, Z.; Mao, B.; Wang, H.; Liu, Z.; Salmeron, M.; Somorjai, G. A. *Chem. Commun.* **2013**, *49*, 6903−6905.

(13) Salmeron, M.; Schlögl, R. *Surf. Sci. Rep.* **2008**, *63*, 169−199.

(14) Zhang, C.; Grass, M. E.; McDaniel, A. H.; DeCaluwe, S. C.; El Gabaly, F.; Liu, Z.; McCarty, K. F.; Farrow, R. L.; Linne, M. A.; Hussain, Z.; Jackson, G. S.; Bluhm, H.; Eichhorn, B. W. *Nat. Mater.* **2010**, *9*, 944−949.

(15) Tao, F.; Grass, M. E.; Zhang, Y.; Butcher, D. R.; Renzas, J. R.; Liu, Z.; Chung, J. Y.; Mun, B. S.; Salmeron, M.; Somorjai, G. A. *Science* **2008**, *322*, 932−934.

(16) Tao, F.; Grass, M. E.; Zhang, Y.; Butcher, D. R.; Aksoy, F.; Aloni, S.; Altoe, V.; Alayoglu, S.; Renzas, J. R.; Tsung, C. K.; Zhu, Z.; Liu, Z.; Salmeron, M.; Somorjai, G. A. *J. Am. Chem. Soc.* **2010**, *132*, 8697−8703.

(17) Hendriksen, B. L. M.; Ackermann, M. D.; van Rijn, R.; Stoltz, D.; Popa, I.; Balmes, O.; Resta, A.; Wermeille, D.; Felici, R.; Ferrer, S.; Frenken, J. W. M. *Nature Chem.* **2010**, *2*, 730−734.

(18) Hendriksen, B. L. M.; Bobaru, S. C.; Frenken, J. W. M. *Surf. Sci.* **2004**, *552*, 229−242.

(19) Zhu, Z.; Tao, F.; Zheng, F.; Chang, R.; Li, Y.; Heinke, L.; Liu, Z.; Salmeron, M.; Somorjai, G. A. *Nano Lett.* **2012**, *12*, 1491−1497.

(20) Völkening, S.; Bedürftig, K.; Jacobi, K.; Wintterlin, J.; Ertl, G. *Phys. Rev. Lett.* **1999**, *83*, 2672−2675.

(21) Michaelides, A.; Hu, P. *J. Am. Chem. Soc.* **2001**, *123*, 4235−4242.

(22) Bedürftig, K.; Völkening, S.; Wang, Y.; Wintterlin, J.; Jacobi, K.; Ertl, G. *J. Chem. Phys.* **1999**, *111*, 11147−11154.

(23) Tao, F.; Tang, D. C.; Salmeron, M.; Somorjai, G. A. *Rev. Sci. Instrum.* **2008**, *79*, 084101.

(24) Grass, M. E.; Karlsson, P. G.; Aksoy, F.; Lundqvist, M.; Wannberg, B.; Mun, B. S.; Hussain, Z.; Liu, Z. *Rev. Sci. Instrum.* **2010**, *81*, 053106.

(25) Finch, G. I.; Murison, C. A.; Stuart, N.; Thomson, G. P. *Proc. R. Soc. London, Ser. A* **1933**, *141*, 414−434.

(26) Gentry, S. J.; Firth, J. G.; Jones, A. *J. Chem. Soc., Faraday Trans.* **1974**, *70*, 600−604.

(27) L'vov, B. V.; Galwey, A. K. *J. Therm. Anal. Calorim.* **2013**, *112*, 815−822.

(28) Powell, C. J.; Jablonski, A. *NIST Electron Inelastic Mean Free Path Database, version 1.2*; National Institute of Standards and Technology: Gaithersburg, MD, 2010.

(29) Norton, P. R. *J. Catal.* **1975**, *36*, 211−223.

(30) Schiros, T.; Näslund, L.-Å.; Andersson, K.; Gyllenpalm, J.; Karlberg, G. S.; Odelius, M.; Ogasawara, H.; Pettersson, L. G. M.; Nilsson, A. *J. Phys. Chem. C* **2007**, *111*, 15003−15012.

(31) Endo, O.; Nakamura, M.; Sumii, R.; Amemiya, K. *J. Phys. Chem. C* **2012**, *116*, 13980−13984.

(32) Yamamoto, S.; Kendelewicz, T.; Newberg, J. T.; Ketteler, G.; Starr, D. E.; Mysak, E. R.; Andersson, K. J.; Ogasawara, H.; Bluhm, H.; Salmeron, M.; Brown, G. E.; Nilsson, A. *J. Phys. Chem. C* **2010**, *114*, 2256−2266.

(33) Yamamoto, S.; Andersson, K.; Bluhm, H.; Ketteler, G.; Starr, D. E.; Schiros, T.; Ogasawara, H.; Pettersson, L. G. M.; Salmeron, M.; Nilsson, A. *J. Phys. Chem. C* **2007**, *111*, 7848−7850.

(34) Andersson, K.; Ketteler, G.; Bluhm, H.; Yamamoto, S.; Ogasawara, H.; Pettersson, L. G. M.; Salmeron, M.; Nilsson, A. *J. Am. Chem. Soc.* **2008**, *130*, 2793−2797.

(35) Casalongue, H. S.; Kaya, S.; Nilsson, A.; Ogasawara, H. Private Communications.

(36) Schauermann, S.; Nilius, N.; Shaikhutdinov, S.; Freund, H.-J. *Acc. Chem. Res.* **2012**, DOI: 10.1021/ar300225s.

(37) Ferrin, P.; Kandoi, S.; Nilekar, A. U.; Mavrikakis, M. *Surf. Sci.* **2012**, *606*, 679−689.

(38) Greeley, J.; Mavrikakis, M. *J. Phys. Chem. B* **2005**, *109*, 3460−3471.

(39) Gland, J. L.; Sexton, B. A.; Fisher, G. B. *Surf. Sci.* **1980**, *95*, 587−602.

(40) Materer, N.; Starke, U.; Barbieri, A.; Döll, R.; Heinz, K.; Van Hove, M. A.; Somorjai, G. A. *Surf. Sci.* **1995**, *325*, 207−222.

12563

dx.doi.org/10.1021/ja406497s | *J. Am. Chem. Soc.* 2013, 135, 12560−12563